

DISCRETE ELEMENT MODELING AND LARGE SCALE EXPERIMENTAL STUDIES OF BOULDERY DEBRIS FLOWS

K.M. HILL^(*), YOHANNES BEREKET^(*), WILLIAM E. DIETRICH^(**), & LESLIE HSU^(**)

^(*) St. Anthony Falls Laboratory, Department of Civil Engineering, University of Minnesota, Minneapolis, MN 55414

^(**) Department of Earth and Planetary Sciences, University of California-Berkeley, Berkeley, CA 94720

ABSTRACT

Bouldery debris flows exhibit a rich variety of dynamics including complex fluid-like behaviour and spontaneous pattern formation. A predictive model for these flows is elusive. Among the complicating factors for these systems, mixtures of particles tend to segregate into dramatic patterns whose details are sensitive to particle property and interstitial fluids, not fully captured by continuum models. Further, the constitutive behaviour of particulate flows are sensitive to the particle size distributions. In this paper, we investigate the use of Discrete Element Model (DEM) techniques for their effectiveness in reproducing these details in debris flow. Because DEM simulations individual particle trajectories throughout the granular flow, this technique is able to capture segregation effects, associated changes in local particle size distribution, and resultant non-uniformity of constitutive relations. We show that a simple computational model study using DEM simulations of a thin granular flow of spheres reproduces flow behaviour and segregation in an experimental model debris flows. Then, we show how this model can be expanded to include variable particle shape and different interstitial fluids. Ultimately, this technique presents a manner in which sophisticated theoretical models may be built which consider the evolving effects of local particle size distribution on debris flow behaviour.

KEY WORDS: debris flow, segregation, simulations, rotating drum, dense granular flows

INTRODUCTION

Bouldery debris flows –consisting of particles ranging from boulders to fine particles with a variety of potential interstitial fluids – are dramatic features in steep upland regions (e.g., IVERSON, 1997) and references within). They play an important role in sculpting the landscape in steep upland regions and have the potential for causing tremendous loss of damage and property (e.g., STOCK & DIETRICH, 2006 and references within). Of additional interest is the wide variety of complex behaviors exhibited by debris flows. They exhibit a rich variety of dynamics including complex solid-like and fluid-like behaviour and dynamic spontaneous examples of pattern formation. Debris flows often start to flow under conditions such as a large rainfall event, but the initiation point is difficult to predict. Once they start to move, they exhibit a variety of behaviours from those similar to a shallow fluid flow, to that of an energetic granular material. Segregation of particles by size mediates the behaviour while the debris flow travels and also in the manner in which it comes to rest. Like a granular material, debris flows stop flowing over a bed of nonzero slope; in other words, they resist macroscopic shear. However, the angle of the slope at which they stop is significantly lower than the measured angle of repose of the debris flow giving rise to a so-called long-runout avalanches (PHILLIPS *et alii*, 2006; LINARES-GUERRERO, 2007). This is likely due in part to a dynamic pore pressure effect giving rise to complex fluid-particle interactions

(e.g., PHILLIPS *et alii*, 2006) but also possibly due to the complex dynamics exhibited by particle mixtures (LINARES-GUERRERO, 2007).

Over the last several decades, there have been a number of approaches to modelling different aspects of debris flows. Examples include non-Newtonian fluid-like models to capture certain details of the constitutive behavior such as the generalized Bingham or Herschel-Buckley model (e.g., IVERSON, 1997 and KAITNA *et alii*, 2007). These models don't take into account the effect of particle size in determining behaviors and therefore are probably most appropriate for debris flows comprised primarily of finer particles or even for the interior of bouldery debris flows where finer particles are most highly concentrated (e.g., IVERSON, 1997). For debris flows where particles are large enough that interparticle collisions become important, interparticle interactions including Coulomb stress and collisional stress appears important for determining internal stress and other details. Collisional stress in sheared granular flows, first modelled by BAGNOLD (1954), has been shown important for determining the behaviour of a wide variety of granular flows (e.g., SILBERT *et alii*, 2001, BREWSTER *et alii*, 2008). Examples for flow in the idealized case where the internal stresses are dominated by Coulomb friction include those by SAVAGE & HUTTER (1989, 1991). IVERSON & DENLINGER (2001, 2004), and others have generalized this to three dimensional flow over rocky terrain.

In addition to the constitutive behaviour of debris flows, recent focus has included the segregation behaviour of mixtures of debris flows consisting of gravels and larger particles where segregation becomes increasingly important in determining local and global constitutive behavior. For example, an apparent feedback mechanism between local particle size distribution and the constitutive behavior appears to be a primary driving mechanism for some pattern formation problems such as a fingering phenomenon observed in some large scale pyroclastic flows (POULIQUEN & VALANCE, 1999).

In channelized debris flows, segregation of the particles by size gives rise to sorted patterns at a variety of length scales that shapes the behaviours of the debris flows. Large particles tend to segregate to the free surface. They also segregate to the front and sides of debris flows. The segregation of large particles to the front gives rise to a course front or "snout" where the particle

size distribution at the front is notably higher than the particle size distribution at the tail. Field and experimental studies of bedrock erosion associated with debris flows indicate that the particle size distribution in the segregated course front or snout plays a significant role in the rate of erosion (STOCK & DIETRICH, 2006, HSU *et alii*, 2008, HSU, 2010). Segregation of the larger particles outward laterally, results in lateral deposits or levees that have a high average particle size compared to that of the body of the debris flow.

Even the particle size in a relatively monosized system affects certain rheological relationships such as the relationship between applied stress and flow rate; segregation affects the local average particle size, so the dynamics of the flow must vary across the debris flow. In other words, it is becoming increasingly clear that one needs to understand the effect of an evolving particle size distribution to develop a predictive model for the dynamics of debris flows when some of the particles are large enough so that interparticle interactions plays an important role in their constitutive behaviours.

There have been a number of modeling techniques used for segregation in dense systems such as that which occurs in debris flows. (See, for example, SAVAGE & LUN, GRAY & THORNTON (2005), and KHAKHAR *et alii* (1997).) The most successful predictive-formulation involves an empirical segregation model superposed on a continuum model for the average flow. Examples include the model first proposed GRAY & THORNTON (2005) (expanded to include diffusion by GRAY & CHUGUNOV, 2006) applied to thin flows in GRAY & ANCEY (2008) and the model of KHAKHAR *et alii* (1997) applied to chaotic flows in a rotating drum by HILL *et alii* (1999). However, these models are not fully predictive in that they employ empirical rules for particle segregation. One of the complicating factors to the application of these models is the degree to which segregation behaviours are sensitive to particle property (HILL & FAN, 2008), interstitial fluid (JAIN *et alii*, 2003), and boundary conditions of granular flows (FAN & HILL, 2010). Currently, there are no physical models that account for these details, only those that account for them in an empirical manner.

Unfortunately, the models for segregation in dense flows are rather limited, and there is precious little investigation as to how the particle size affects important rheological relationships. An alternative approach to a continuum model for understanding-

segregation and other details of particle interactions in debris flows is the Discrete Element Method (DEM). First proposed in the late 1970's by Cundall and Strack, the DEM approach has the capability of tracking individual particles throughout a simulation. Rather than a bulk model for rheological relationships, the DEM approach relies on simple models describing interactions between particles and then obtains the resulting motion through numerical integration of the accelerations of the particles derived from the total force on each particle, as detailed in the next section. The technique therefore has the capability of capturing segregation effects and subsequent changes in the local rheological behaviour of a particulate flow and even forces and stresses between the particles and the boundary rather than imposing rules based on, for example, empirical data. In this paper, we first provide an overview of the DEM for dry granular flows. Then we present results comparing data from these DEM simulations with model experimental debris flows and discuss how the DEM simulations can be made to more realistically represent debris flows.

DISCRETE ELEMENT METHOD SIMULATIONS

Modelling granular materials using the DEM method was first proposed by CUNDALL & STRACK (1979). The DEM method is in many ways similar to Molecular Dynamics (MD), (e.g., ALLEN, 2004), though in contrast to MD simulation, individual macroscopic particles rather than molecules are treated as distinct objects; in other words, the interaction between two particles is modelled as a single force (rather than a sum of all the molecular forces associated with atoms and molecules composing each particle). Additionally, in DEM simulation of macroscopic dry granular systems, only particles in direct contact with one another interact and may repel and rotate one another.

DEM models vary in how they treat the forces between particles. In our simulations, we use what is called a "soft sphere" model (e.g., CUNDALL AND STRACK, 1979, TSUJI *et alii*, 1992) which takes into consideration the deformation that occurs over time during particle-particle interactions. While this detail is not always important for relatively sparse granular materials where interparticle interactions are relatively rare and typically binary, the details of interpar-

ticle interaction are of critical importance for dense granular systems where particles undergo enduring interaction with one another, often with more than one particle at a time.

As is typical, in our soft sphere DEM model, when two particles come into contact, their deformations are modelled with an effective overlap between the particles (Fig. 1). The force exerted by the particles on one another is estimated based on the effective deformation or overlap of each particle in contact. The resulting interparticle force is dependent on the magnitude and rate change of the overlap tangential and normal to the line connecting the particles. This may be thought of as a relative movement of the contact points between the particles normal and tangential to the plane of overlap, δ_n and δ_t , respectively.

The force model consists of two parts in each direction: a nonlinear restorative spring, dependent only on the amount of deformation or overlap, and a damping mechanism, dependent on the rate change of deformation or overlap:

$$F_n = k_n \delta_n^{3/2} + \gamma_n \delta_n^{1/4} \dot{\delta}_n$$

$$F_t = \min \left\{ k_t \delta_n \delta_t^{1/2} + \gamma_t \delta_n \dot{\delta}_t^{1/2}, \mu F_n \right\} \quad (1)$$

Here, the subscripts n and t indicate normal components and tangential components of each parameter respectively. F_n and F_t represent the normal and tangential components of the forces as previously de-

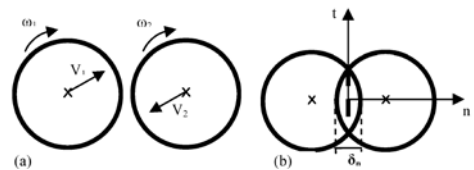


Fig. 1 - Illustration of the interaction of two particles in a soft sphere DEM model. (a) Two particles approach each other at velocities of V_1 and V_2 and rotational speeds of ω_1 and ω_2 . (b) During collision the particles the deformation is represented by the normal overlap (δ_n) between the two circular particles. The plane of contact is assumed to be flat and perpendicular to the line joining the centers of the two particles. n is the axis perpendicular (normal) to the contact plane and t is the axis parallel (tangential) to the contact plane in the direction of relative movement normal to n . $\dot{\delta}_t$ is not shown

scribed. k_n and k_t are the stiffness factors of particles, δ_n and δ_t are the overlaps between particles and γ_n and γ_t are the damping factors. μ is the coefficient of friction between the interacting particles

The exponents and stiffness factors of particles k_n and k_t are based on Hertzian contact theory (HERTZ, 1896) and MINDLIN & DERESIEWICZ (1953):

$$k_n = (4/3)\sqrt{R_{eff}}E_{eff}$$

$$k_t = 8\sqrt{R_{eff}}G_{eff} \tag{2}$$

Where R_{eff} is the effective radius of the two particles in contact, E_{eff} is their effective modulus of elasticity, and G_{eff} is their effective shear modulus:

$$R_{eff} = (1/r_1 + 1/r_2)^{-1}$$

$$E_{eff} = ((1 - \nu_1^2)/E_1 + (1 - \nu_2^2)/E_2)^{-1} \tag{3}$$

$$2G_{eff} = ((1 + \nu_1)(2 - \nu_1)/E_1 + (1 + \nu_2)(2 - \nu_2)/E_2)^{-1}$$

Here, the subscript refers to one of the two particles in contact, and r_i , ν_i , E_i are the radius, Poisson's ratio, and modulus of elasticity of particle i , respectively

There is no simple theoretical description for the damping component. We use the following form similar to TSUJI *et alii* (1992):

$$\gamma_n = \alpha\sqrt{m_{eff}k_n} \tag{4 a}$$

$$\gamma_t = \alpha\sqrt{m_{eff}k_t} \tag{4 b}$$

where m_{eff} is the effective mass of two particles in contact: $m_{eff} = (1/m_1 + 1/m_2)^{-1}$, and α varies with the coefficient of restitution according to the numerical solution by TSUJI *et alii* (1992).

The force model for interactions between particles and other objects (such as container boundaries or walls) is similar to the inter-particle force model described by Equations 1(a) and 1(b). The dimensions of the walls are usually much larger than the particle sizes, so wall mass and radius are considered infinite. Therefore, the effective radius during a particle-wall contact is considered equal to the radius of the particle.

Based on the individual contact forces between all particles (and, where appropriate, the walls) and the masses of those particles, we calculate the net force and net moment on each object and, from this, the

translational and rotational accelerations using Newton's and Euler's second laws. We use the Fourth Order Runge Kutta numerical scheme to integrate the particle accelerations to determine the rotational and translational velocities and displacement of the particles at each instant in time. To assure numerical stability we use a time step of approximately 1.4 μ s for these calculations (MUNJIZA, 2004).

PRELIMINARY RESULTS: DRY SPHERICAL PARTICLES IN A DRUM

For this paper, the boundary conditions of our simulations were modelled after an experimental drum used for studying model debris flows at the University of California at Berkeley described in detail in Hsu *et alii*, (2008). The drum diameter $D = 0.56$ m and its width $w = 0.15$ m. The front vertical wall is made of clear acrylic, so quantities such as surface profile and particle location for those particles adjacent to the wall are accessible. The flat vertical sidewalls are relatively smooth. For the experiments described here, the outer curved boundary over which the particles move – i.e., the bed – was roughened with attached sandpaper but otherwise is not bumpy.

The drum has the capacity to house erodible panels at the “bed” of the model debris flows, though for this paper we focus instead on the kinematic behaviour of the particles. For this, we model thebehaviour of 13.8mm spherical glass marbles that were sheared in the experimental drum and also the behaviour of very simple mixtures – a single larger particle among the 13.8mm particles. The 13.8 mm “matrix” particles had a measured polydispersity of 10%, so in reality they ranged from approximately 12.4 mm – 15.2 mm.

The simulated particles were given the properties of quartz, similar to those typical of glass. The properties are shown in Table I. In all cases, the particles may be considered in the hard sphere limit as we discuss in Hill and Yohannes (2010, under review). The particle

material density $\rho=2650$ kg/m ³
modulus of elasticity $E=29$ GPa
Poisson's ratio $\nu=0.15$
coefficient of friction between particles $\mu_{PP} = 0.5$
coefficient of friction between a particle and the bed $\mu_{PB} = 0.7$
coefficient of restitution $e \sim 0.89$

Tab. 1 - Properties of the simulated particles

sizes we use in the simulations are again identical to those in the physical experiments: $d = 13.8 \text{ mm} \pm 10\%$ for most of the experiments. The values of the numerical parameters for the nonlinear force model between individual particles [Equation 2(a) and 2(b)] were derived from the formulas detailed in the previous section.

The model drum has dimensions identical to that of the experimental drum: $D=0.56 \text{ cm}$ and $W = 0.15 \text{ cm}$. The walls of the drum are physically smooth (i.e., without bumps), and the wallparticle frictional coefficient is slightly greater than that between particles to account for the additional friction associated with the sandpaper. All other material properties of the walls are the same as that for the particles. Snapshots from one of these computational experiments are shown in Fig. 2.

Particle trajectories in the experimental and computational drums follow similar 3-dimensional circulation patterns. Particles in contact with the bed and walls are dragged upstream in the direction of the walls, though there is some slip between the walls and the particles so that the particles immediately adjacent to the walls are not dragged as quickly upstream as the bed is moving. The particles adjacent to the bed are carried to the back where they then flow down the top surface of the particles. In other words, the top and bottom surfaces move like two sides of a conveyor belt relative to one another. From a plan view, lateral motion toward

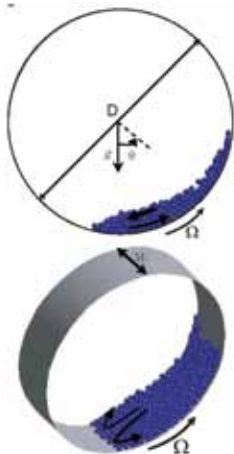


Fig. 2 - Snapshots from two different perspectives from an instant in time from a simulation performed modeled after physical experiments in the drum described in the text with 3.13 kg of 13.8 mm spherical glass particles. Rotation direction indicated by the vectors outside of the drums. Movement of the particles indicated by arrows drawn over the beads

the side walls occurs at the front of the flow, analogous to the motion associated with levy formation in debris flows in nature. Individual particle trajectories in this general circulation pattern vary depending on particle size, as we describe shortly.

Since the flow in both the experimental and computational drum is shallow, the entire depth of the flow is sheared, and there is no plug-like section that is common in deeper flows. From the side view, there is a steady, spatially varying velocity field from the top to the bottom of the flow between the upstream and downstream moving particles. The movement of the particles in the drum is analogous to that the flow of particles down a hillslope, with two chief exceptions. First, the hillslope is stationary, so none of the particles are moving backwards except in a relative sense, for example, to the direction of motion of the particles on the top of the debris flow. Second, the bed at the back of the flow in the drum reaches unreasonably high slopes compared to that of real debris flows. We limit ourselves to the front and middle of the flow in the drum for making analogies to real debris flows.

In Figures 3 and 4 we compare some data from the physical and computational experiments. Fig. 3 shows sample surface profiles derived experimentally (a) and computationally (b) and (c) for the same mass of 13.8 mm spherical glass particles (3.13 kg). As qualitatively apparent from the snapshots in Fig. 2, the model debris flows are bulky at the front and diminish toward the back. The similarity between the results from the physical and computational models over the whole field of particles gives credence to the effectiveness of the DEM simulations in modelling these systems. The

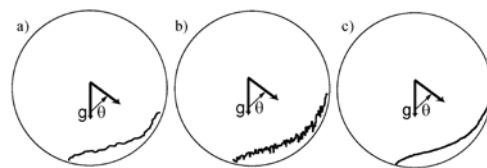


Fig. 3 - Surface profiles of the particles in the physical and computational experiments described in the text. (a) the longitudinal profile from the physical experiments at one instant in time. (b) the same from the computational experiments. (c) the average over 20 rotations from the computational experiments

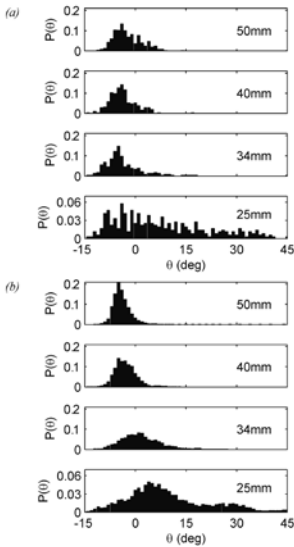


Fig. 4 - Results from (a) physical and (b) computational experiments using particles of total mass 3.13 kg rotated in a drum of dimensions $D = 0.56m$, $w = 0.15m$. The particles in each experiment consisted of a single large particle (size indicated in the figures) in a matrix of 13.8 mm particles. The plots are the probability distribution function (pdf) of the location of the large intruder particle. Please see Figs. 2 and 3 for definition of θ

similarity of the profiles indicate the internal stresses of the bulk granular flow are well-represented by the interparticle force model within the DEM simulation.

In a mixture, the behaviour of the particles is similar to that described above and shown in Figs. 2 and 3, but there are marked differences in the behaviour of individual particles that vary with particle size. For example, while larger particles roughly follow the circulation of the general flow at the front, once they start to move back, they quickly segregate upward toward the free surface, as is typical of mixtures of different sized particles (e.g., KHAKHAR *et alii*, 1997). Once at the top, the large particles follow the trajectories of their new neighbors at the top of the flow and return to the front.

This results in a higher concentration of large particles at the front of the flow than their representative concentration in the bulk. Particles that are only moderately larger than their neighbors take longer to segregate to the free surface and therefore, they typically have a higher concentration slightly further back in the flow. In other words, while the segregation behaviour is similar for all larger particles, it is most dramatic for the largest particles. The relationship between this segregation pattern and particle size is

complicated (e.g., FÉLIX & THOMAS, 2004).

We performed simple experiments and simulations to validate sorting effects in the simulation using “mixtures” consisting primarily of 13.8mm spherical “matrix” particles and a single larger “intruder” particle. We kept the mass constant for each mixture so that in each case a quantity of matrix particles whose mass equalled that of the intruder particles was removed. Figure 4 illustrates the longitudinal position of relatively large intruder particles using a probability distribution (pdf) of the intruder particle in each case. Similar to large-scale bouldery debris flows with a much wider particle size distribution, the large particles are found toward the front of these physical (Fig 4.a) and computational (Fig. 4.b) model debris flows. The top figure in each pair shows the pdf of the intruder particle location for the experiments using a single 50 mm spherical particle among the 13.8 mm particles. The next three rows show results the same total mass of particles, but the size of the intruder particle decreases in each subsequent panel to 40mm, 34mm, and then 25mm.

For the 50 mm intruder particle experiments and simulations, the peak is near $\theta = -5^\circ$, i.e., near the front of the flow, and relatively narrow. For smaller intruder particles (though still larger than the matrix particles), the peak broadens, and the tail of the distribution thickens toward the back of the flow. For the 25 mm intruder particle experiments and simulations, the front peak is notably farther back and broader, and there appears to be a secondary peak two thirds of the way back in the flow. (The latter is likely related to the complications that arise from the anomalously high slopes and not relevant for real debris flows).

Admittedly, there are also a few differences between experiments and simulations. The experimental results are somewhat noisier and the peaks are broader. We believe these differences are primarily due to subtle differences between the physical experiments and the simulations. First, the simulated particles do not capture all details of the experimental particles which are slightly aspherical and have slight asperities. The experimental drum also is not perfectly true as it is in the simulations. Finally, while we can follow a particle throughout the simulations, no matter where it is located, we can only see the particles in the physical experiments if they are immediately adjacent to the wall. However, we feel the trends are similar enough to say that trends associated with particle size distribution are

captured well by the simulations

While the results obtained show promise for capturing certain qualitative details of model debris flows, there are several simplifications in the simulations compared with real debris flow systems. We are currently working to build the level of sophistication of our model to address some of the more complicated effects. We describe our efforts in the next section..

ADDITIONAL EFFECTS: PARTICLE SHAPE AND INTERSTITIAL FLUIDS

The simulations described in the previous two sections are performed using dry spherical particles. However, particles in natural debris flows are aspherical, real debris flows involve particles that are distributed over a wide range of particle size and involve millions of particles, and typically interstitial fluid influences the behaviour of debris flows through effects such as cohesivity and pore pressure. While current computational power limits the number of particles that we can simulate, we can address some of the other issues through various computational techniques. We describe our preliminary efforts to simulate debris flows that have aspherical particles and interstitial fluids that alter the dynamics of the flow briefly in this section

PARTICLE ASPHERICITY IN DEBRIS FLOWS

In reality, unlike the particles in the model described above, the particles that compromise the granular materials in debris flows are, in general, aspherical. Compared with aspherical particles, spherical particles tend to roll and slide past other spherical particles relatively easily. This difference leads to discrepancies in bulk macroscopic properties and is generally believed to cause an unphysically low stiffness in some DEM models (TANAKA *et alii*, 2001 and TING *et alii*, 1995), subsequently, an unreasonably low angle of repose (CALANTONI *et alii*, 2004). A number of different techniques have been used to represent the effect of the asphericities.

There are two primary techniques used for modelling aspherical particles. One is through the modification of the shape of the primary entities of the particles from spheres to aspherical particles. This requires changing the algorithm and force contact model described above depending on the orientation of the particles. The most widely used aspherical particle shape for DEM simulations is an ellipse (TING *et alii*, 1995).

Other DEM modellers used polygons to generate rougher form of asphericity, such as those described in ULLDITZ (2001). However, the singularity problem at the corners of the polygon makes this method difficult to implement efficiently. Further, both methods for representing aspherical particles in DEM simulations take significant additional computational time.

The second common approach used for modelling nonspherical, irregularly shaped particles involves what one might call “computationally gluing” spherical particles together (THOMAS & BRAY, 1999; ZEGHAL, 2001; CALANTONI *et alii*, 2004; YOHANNES, 2008). In other words, multiple spherical particles are attached to one another into a rigid-body cluster. When a sphere in one cluster contacts a sphere in another cluster, the forces between them are calculated as if they were individual spheres using Equations 1(a) and 1(b). The primary difference between simulations involving single spherical particles and these aspherical particles comprised of clusters of spherical particles arises from the calculation of the kinematics of the aspherical particle clusters. To calculate the movements of the particle clusters at each time step, first all the forces on all particles in a cluster are used to calculate the resultant force for the cluster and the resultant force moment about the mass center of the cluster. Then, the rotational and translational acceleration of each individual particle cluster is determined from the force and force moments using the cluster mass and moment of inertia of each cluster particle.

There are several benefits to this last method of generating aspherical particles. Gluing spherical particles offers flexibility without significant additional computational cost. Any number of particles with different sizes can be glued together to form a wide variety of particle shapes. (A few are illustrated in Fig. 5.) CALANTONI *et alii* (2004) showed that by using aspherical particles consisting of as few as 3 glued spheres per cluster, one can reproduce such macroscopic

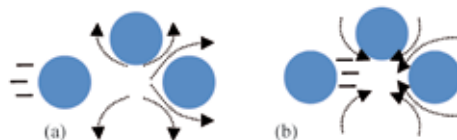


Fig. 5 - Particles that may be created from glued spherical particles that (a) may not or (b) may overlap, and (c) may even be of different sizes

measures of the internal stress of the materials such as the angle of repose. In addition, inter-particle contact detection can be performed easily, and calculating interparticle forces is simply a matter of using the equations described above for spherical particles, though in the case of the clusters, one must consider contacts between individual particles in a one cluster with those in another. Admittedly, there is additional computational time associated with the number of particles in a cluster. Nevertheless, the computational time requirement is significantly less than other methods for simulating aspherical particles described above.

We have found simulating aspherical particles by using glued clusters of particles in pairs or in triplets to sufficiently reproduce tests of the strength of materials, as described in YOHANNES (2008). We are currently using this approach to investigate the effect particle asphericity on the kinematics of gravity-driven debris flows.

INTERSTITIAL FLUIDS IN DEBRIS FLOWS

In addition to particle shape, it is well known that interstitial fluid plays an important role in most granular flows. The presence of a fluid introduces a cohesivity between particles, provides lubrication allowing particles to more easily slide past one another, and can be the source of anomalous effects associated with pressure in the fluid that is greater than the hydrostatic pressure. Modelling these effects are somewhat more complicated than modelling dry particles alone as they involve longer-range interactions between particles.

In this section we present two methods we are investigating for their effectiveness in modelling the presence of an interstitial fluid in debris flows and some preliminary results from simulations employing these methods. In each case, we investigate a method for reproducing the effect of a fluid at the scale of particle-particle interactions and investigate the resulting change in dynamics at the scale of the system.

MODELING COHESION ASSOCIATED WITH INTERSTITIAL FLUIDS

When the pore spaces between the particles are not entirely filled with water, the effect of an interstitial fluid at the scale of individual particles is primarily associated with a cohesivity between particles that is not present in dry granular materials (e.g., MASON

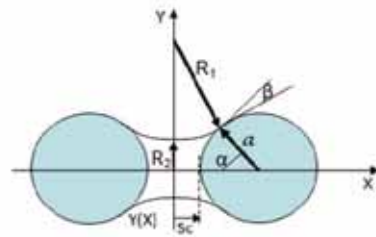


Fig. 6 - Liquid bridge between two spherical particles. R1 and R2 are the longitudinal and meridian radius of the curvature of the surface of liquid

& CLARK, 1965; MELROSE, 1966; GILLESPIE & SETTINERI, 1967; HO’ITA *et alii*, 1974). The liquid forms what is referred to as a ‘liquid bridge’ between pairs of closely-spaced particles, as sketched in Fig. 6. Liquid bridges are responsible for an apparent attractive force between neighboring particles associated with two effects: (1) the surface tension of the interstitial fluid and (2) the pressure gradient between the fluid in the liquid bridge and the “void space,” occupied by air (HO’ITA *et alii*, 1974). The resulting force F_c can be modelled as detailed in HO’ITA *et alii* (1974):

$$F_c = \pi(d/2)^2(\Delta P_c)\sin^2(\alpha) + \pi d\Gamma \sin(\alpha)\sin(\alpha + \beta) \quad (6)$$

Where Γ is the surface tension of the interstitial fluid, d is the particle diameter, a is the half filling angle and β is the contact angle between the liquid and a particle (please see Fig. 6). ΔP_c is the pressure difference between the inside of the liquid bridge and the atmosphere (determined by the radius of curvature of the liquid bridge), and is computed from the Laplace-Young equation:

$$\Delta P_c = \left(\frac{1}{R_1} + \frac{1}{R_2}\right)\Gamma = Y' \left(\frac{Y''}{(1+Y'^2)^{3/2}} - \frac{1}{Y(1+Y'^2)^{1/2}}\right)\Gamma \quad (7)$$

where R1 is the meridian radius of curvature, and R2 is the minimum width of the liquid bridge. Y' is the spatial derivative of Y with respect to X, and Y'' is the spatial derivative of Y' with respect to X. The size of each liquid bridge is determined by the level of saturation and the number of particles close enough for liquid bridges to form. The effect of the liquid bridges is more pronounced on smaller size particles (maximum size of about 2 mm). Therefore for bouldery debris flows this method is primarily helpful for understanding the effect of cohesivity on debris flows. Previously,

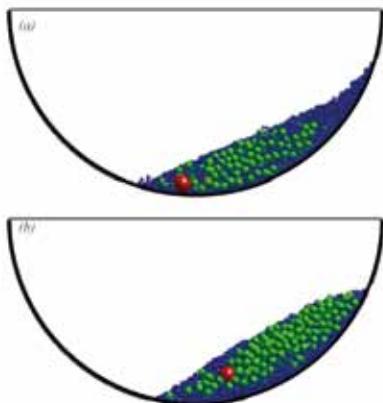


Fig. 7 - Snapshots from simulations of relatively small particles (a) without interstitial fluid and (b) with 10% interstitial fluid. In both case, the drum diameter $D = 140$ mm; the drum thickness: $w = 37.5$ mm; and the particle diameters are: 1.25 mm, 3.0mm and 6.25mm; total mass of particles: 0.0524 kg; rotational speed: 48 rpm

in other contexts, cohesivity has been shown to have a strong effect on details such as particle segregation (LI & MCCARTHY, 2005) and shear strength of granular materials (LIU & SUN, 2002). We investigate the effect for thin granular flows by simply considering the force associated with Equation (6) (with the solution for pressure difference described by Equation (7)) as an additional normal force between separated particles.

Figure 7 shows a snapshot from a mixture of three different sized particles when there is no interstitial fluid and when there is 10% water in among relatively small particles. The picture is representative of a near steady state for both systems. Two differences are apparent. First, the segregation is clearly affected by the presence of liquid. In the case of the system shown in Fig. 7(b), the larger particles no longer segregate all the way to the front of the flow. Second, the longitudinal profile is altered, suggesting the internal stresses of the granular assembly as a whole are affected by the local interactions between individual particles.

Figure 8 shows the steady state velocity profiles for the model systems depicted in Fig. 7. Figure 7(a) is the profile of the particles alone, while Fig. 7(b) shows the profile for the case with some fluid. The fluid in this case reduces the maximum velocity and the average shear rate by approximately 1/3. All of this information is useful in considering the possible modifications one could make to continuum models for particle/fluid mixtures. However, additional ef-

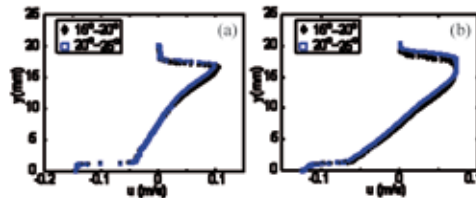


Fig. 8 - Velocity profiles from two different locations in the model debris flows depicted in Fig. 7(a) without and (b) with 10% interstitial fluid. Results from two different positions in the drum are shown for values of θ indicated in the legend. (Please see Figs. 2 and 3 for definition of θ)

fects are apparent from pore pressure effects as we address in the next subsection.

HIGH MOISTURE CONTENT

When the pore spaces between the particles are entirely filled with liquid, the effect the liquid has on the interparticle interactions is not limited to cohesivity. The large-scale mechanics of the particle-fluid interactions in this case are not fully understood, but they are generally linked to the effect of the variability of pore pressure (e.g., SASSA, 1984; GABET & MUDD, 2006; DEANGELI, 2009; IVERSON *et alii*, 2000).

To understand this, we first consider a static system of macroscopic particles where the spaces among particles are mutually connected and entirely filled with a liquid. In this case, the pressure in the liquid, the pore pressure, is typically equal to what it would be in a static fluid, its hydrostatic pressure: $p_h = \rho_L gh$, where ρ_L is the density of the liquid, g is gravitational acceleration, and h is depth beneath the free surface. However, in a sheared (or in some case, even slightly disturbed) fluid-particle flow the pore pressure can increase in part due to relative fluid and particle motion. In addition to their movement associated with the average flow, particles tend to approach and recede from one another. The presence of liquid in the pores dampens this somewhat, particularly when the liquid is unable to move through the pores rapidly enough to accommodate relative particle movement. This tends to reduce contact between particles. When this happens, the interstitial liquid rather than interparticle contacts supports the particles, resulting in pore pressure in excess of hydrostatic pressure.

This can result in dramatic differences in the behaviour of the debris flow including increased mobility leading to long run-out avalanches (CASAGRANDE,

1971; WANG & SASSA, 2003; SASSA & WANG, 2003; OKADA & OCHIAI, 2008; DEANGELI, 2009). There are a number of details that moderate the degree to which excess pore pressure occurs and influences the behaviour of a debris flow, particularly factors that modify the permeability including void ratio, particle size distribution of the granular material and fine particle content (WANG & SASSA, 2003). A reduced permeability impedes both the movement of fluid and, correspondingly, the dissipation of excess pore pressure generated due to some deformation in saturated granular materials. To better understand the effects of the pore-pressure on flow properties, models that account specifically for the modified particle-particle and particle-fluid interactions are helpful.

To develop such a model, we consider Fig. 9 which illustrates the dynamics that can lead to increased pore pressure for a single particle approaching or departing from a group of other particles. A particle approaching a group of other particles needs to push out a pocket of interstitial fluid and thus that particle and the group of particles feels a mutually repellent force. DEM models that incorporate this effect of pore pressure have been proposed by TARUMI & HAKUNO (1988) and OKADA & OCHIAI (2007). These models are based on tracking the change in the pore spaces between particles. For example, if volume of a pore space decreases, the pressure gradient forces the fluid to flow to adjacent pore spaces. These models were capable of demonstrating the evolution of pore-pressure associated with applied stresses in saturated granular materials. However, tracking the pore spaces in DEM models is computationally very intense and these two DEM models are limited to 2D set up or to a very few particle in 3D. This makes their implementation into debris flow models impractical.

We suggest a simpler model to capture the essence of the effect of pore pressure without as much additional computational intensity. This model captures the “action at a distance” for particles moving relative to one another as suggested by the sketches in Fig. 9. As we noted above, the presence of fluid dampens relative particle motion for particles in close proximity. A model that captures this basic idea can be written as follows:

$$\vec{F}_{12} = -k\vec{v}_n/r_{12} \quad (8)$$

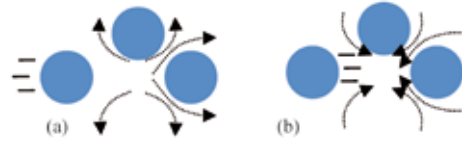


Fig. 9 - Sketches illustrating the effect of a pore-filling liquid on damping relative particle motion. The liquid can either work to create a repulsive force between particles if they are approaching or to effectively attract them if they are moving away from one another

where in suggesting this, we propose that \vec{F}_{12} , the fluid-mitigated force associated with two nearby particles moving relative to one another, increases as their relative velocities increase and decreases with distance to one another. \vec{v}_n is their relative velocity in the direction connecting their two particle centres (this is similar to the definition of δ_n of Equation 1(a), though here the particles are not necessarily touching); r_{12} is the distance between particle centres, and k can be thought of as a “pore pressure coefficient” that varies with fines content and other details that influence the permeability of the particle network. We expect k to vary with details of the system including fines content and more general considerations of the particle size distribution.

The model described by Equation 8 is completely phenomenological, and we expect it to be modified with more detailed comparisons with experimental and field data. We consider it a first order attempt to represent the action at a distance brought about by the saturated interstitial fluid in a DEM that facilitates investigations of this effect on larger systems.

Figure 10 shows data comparing the velocity profile from a dry system with one where the fluid saturates the system as modelled by Equation 8. Figure 10(a) shows the velocity profile of a system that does not include consideration of any fluid effects and is thus fully represented by Equation 1 and Fig. 10(b) includes the additional normal force described in (8) added to Equation 1(a). For the system where an extra term is added to account for pore pressure effects, the flow is slowed by approximately 30%. More notably, however, there is a qualitative difference with the additional pore pressure effect. The flow profile concavity has changed and it resembles slightly more the plug flow expected by excess pore pressure effects and observed in experimental flows in large scale experimental drums.

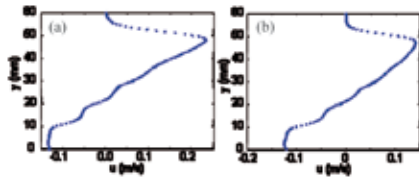


Fig. 10 - Velocity profiles from model debris flows where particle interactions are modelled as (a) dry, completely described by Equation (1) and (b) saturated, where the additional long range force described by Equation (8) is added to the normal force

DISCUSSION AND CONCLUDING REMARKS

The first results of this preliminary model for debris flow capture a number of important details from debris flows including the following:

Individual particles segregate according to size from front to back in a thin sheared granular flow;

Larger particles segregate to the front. This trend decreases systematically with particle size relative to the size of particles in the bulk;

The longitudinal profiles from the simulations were similar to that from experiments comprised of dry spherical particles, suggesting that the constitutive behaviour is well-represented by the DEM model; While the results of this model to date are primarily from dry flow of spherical particles, implementation of additional modelling techniques show promise for simulating more sophisticated flows. These include more details associated with realistic particles and in-

terstitial fluids more common in natural debris flows. Ongoing work includes the following:

Investigation of the effect of particle shape on flow behaviour

Investigation of the influence of the effects of cohesivity and action at a distance associated with interstitial fluids Initial comparison of these results with large scale experiments with aspherical particles and different interstitial fluid is ongoing. Preliminary results indicate the simple modifications suggested in this paper have potential for reproducing some of the complicated effects in natural debris flows. In the long run, results from Fig. 10 Velocity profiles from model debris flows where particle interactions are modelled as (a) dry, completely described by Equation (1) and (b) saturated, where the additional long range force described by Equation (8) is added to the normal force. (a) (b) simulations such as those described here can inform the development of sophisticated continuum models for debris flows that better represent evolving particle size distributions and solid and fluid concentrations.

ACKNOWLEDGEMENTS

Support for this research was provided in part by the University of Minnesota and the University of California – Berkeley, and by the National Center for Earth Surface Dynamics (NCED), a NSF Science and Technology Center funded under agreement EAR-0120914.

REFERENCES

- BAGNOLD R.A. (1954) - *Experiments on a gravity-free dispersion of large solid spheres in a Newtonian fluid under shear*. Proc. Roy. Soc. London. Series A, **225**(1160): 49-63.
- BREWSTER R., SILBERT L.E., GREST G.S. & LEVINE A.J. (2008) - *Relationship between interparticle contact lifetimes and rheology in gravitydriven granular flows*, Phys. Rev. E, **77**: 061302.
- CALANTONI J., HOLLAND K.T. & DRAKE T.G. (2004) - *Modelling sheet-flow sediment transport in wave-bottom boundary layers using discreteelement modelling*. Philos. Transact A Math Phys Eng Sci., **362**: 1987-2001.
- CASAGRANDE A. (1971) - *On liquefaction phenomena*. Geotech., **21**(3): 197-202.
- CUNDALL P.A. & STRACK O.D.L. (1979) - *A discrete numerical model for granular assemblies*. Géotechnique, **29** (1): 47-55.
- DEANGELI C. (2009) - *Pore water pressure contribution to debris flow mobility*. American Journal of Environmental Sciences, **5** (4): 486-492.
- DENLINGER R.P. & IVERSON R.M. (2004) - *Granular avalanches across irregular three-dimensional terrain: I. Theory and computation*. J. Geophysical Research, **109**: F01014, doi:10.1029/2003JF000085.
- FAN Y. & HILL K.M. (2010) - *Shear-driven segregation of dense granular mixtures in a split-bottom cell*. Phys. Rev., **E 81** (11): 041303.
- FÉLIX J. & THOMAS N. (2004) - *Evidence of two effects in the size segregation process in dry granular media*. Phys. Rev., **E 70**: 051307.

- GABET E.J. & MUDD S.M. (2006) - *The mobilization of debris flows from shallow landslides*. *Geomorphology*, **74**: 207-218.
- GILLISEPIE T. & SETTINERI W.J. (1967) - *The effect of capillary liquid on the forces of adhesion between spherical solid particles*. *J. Colloidal and Interface Science*, **24**: 199-202.
- GRAY J.M.N.T. & ANCEY C. (2008) - *Segregation, recirculation and deposition of coarse particles near two-dimensional avalanche fronts*. *J. Fluid Mech.*, **629**: 387-423.
- GRAY J.M.N.T. & CHUGUNOV V.A. (2006) - *Particle-size segregation and diffusive remixing in shallow granular avalanches*. *J. Fluid Mech.*, **569**: 365-398.
- GRAY J.M.N.T. & THORNTON A.R. (2005) - *A theory for particle size segregation in shallow granular free-surface flows*. *Proc. R. Soc. A*, **461**: 1447-1473.
- HERTZ H. (1896) - *Über die berührung fester elastischer Körper* (On the contact of rigid elastic solids). In: *Miscellaneous Papers*. JONES & SCHOTT, EDITORS, *J. reine und angewandte Mathematik* 92, Macmillan, London (1896), p. 156 English translation: Hertz H.
- HILL K.M., KHAKHAR D.V., GILCHRIST J.F., MCCARTHY J.J. & OTTINO J.M. (1999) - *Segregation driven order in chaotic granular flows*. *Proc. Nat. Acad. Sci.*, **96** (21): 11701-11706.
- HILL K.M., GIOIA G. & AMARAVADI D. (2004) - *Radial segregation patterns in rotating granular mixtures: waviness selection*. *Phys. Rev. Lett.*, **93**(22): 224301.
- HILL K.M. & FAN Y. (2008) - *Isolating segregation mechanisms in a split-bottom cell*. *Phys. Rev. Lett.*, **101** (8): 088001.
- HOITA K., TAKEDA K. & IINOYA K. (1974) - *The capillary binding force of a liquid bridge*, *Powder Tech.*, **10**: 231-242.
- HSU L. (2010) - *Bedrock Erosion by Granular Flow*, PhD thesis, University of California, Berkeley.
- HSU L., DIETRICH W. E. & SKLAR L. (2008) - *Experimental study of bedrock erosion by granular flows*, *J. Geophysical Research*, **113**: F02001
- IVERSON R.M. & DENLINGER R.P. (2001) - *Flow of variably fluidized granular masses across three-dimensional terrain, I. Coulomb mixture theory*. *Journal of Geophysical Research*, **106**(B1): 537-552.
- IVERSON R.M., REID M.E. & LAHUSEN R.G. (1997) - *Debris-flow mobilization from landslides*. *Annual Reviews of Earth and Planetary Science*, **25**: 85-138.
- IVERSON R.M., REID M.E., IVERSON N.R., LAHUSEN R.G., LOGAN M., MANN J.E. & BRIEN D.L. (2000) - *Acute sensitivity of landslide rates to initial soil porosity*. *Science*, **290**: 513-516.
- JAIN N., OTTINO J.M. & LUEPTOW R.M. (2003) - *Effect of interstitial fluid on a granular flowing layer*. *J. Fluid Mech.*, **508**: 23-44.
- KAITNA R., RICKENMANN D. & SCHATZMANN M. (2007) - *Experimental study on rheologic behaviour of debris flow material*. *Acta Geotechnica*, **2**(2): 71-85.
- KHAKHAR D.V., MCCARTHY J.J. & OTTINO J.M. (1997) - *Radial segregation of granular mixtures in rotating cylinders*. *Phys. Fluids*, **9** (12): 3600-3612.
- LINARES-GUERRERO E., GOUJON C. & ZENIT R. (2007) - *Increased mobility of bidisperse granular flows*. *J. Fluid Mech.*, **593**: 475-504.
- MASON G. & CLARK W.C. (1965) - *Liquid bridges between spheres*. *Chem. Eng. Sci.*, **20**: 859-866.
- MELROSE J.C. (1966) - *Model calculations for capillary condensation*. *AIChE J.*, **12**: 986-994.
- MINDLIN R.D. & DERESIEWICZ H. (1953) - *Elastic Spheres in Contact under Varying Oblique Forces*. *J. Applied Mechanics*, **20**(3): 327-344.
- MUNJIZA A. (2004) - *The Combined Finite-Discrete Element Method*. John Wiley & Sons, Inc., West Sussex.
- OKADA Y. & OCHIAI H. (2007) - *Coupling pore water pressure with distinct element method and steady state strengths in numerical triaxial compression tests under undrained conditions*. *Landslides*, **4**: 357-369.
- OTTINO J.M., & KHAKHAR D.V. (2000) - *Mixing and segregation of granular materials*. *Annual Review of Fluid Mechanics*, **32**(1): 55-91.
- PHILLIPS J.C., HOGG A.J., KERSWELL R.R. & THOMAS N.H. (2006) - *Enhanced mobility of granular mixtures of fine and coarse particles*. *Earth Planet Sci. Lett.*, **246**: 466-480.
- POULIQUEN O. & VALLANCE J.W. (1999) - *Segregation induced instabilities of granular fronts*. *Chaos*, **9**(3): 621-630.
- SARKAR S. & KHAKHAR D.V. (2008) - *Experimental evidence for a description of granular segregation in terms of the effective temperature*. *Europhysics Letters*, **83**: 5400.

- Sassa, K., (1984) - *The mechanism starting liquified landslides and debris flows. 4th International Symposium on Landslides.* International Society for Soil Mechanics and Foundation Engineering, Toronto, Ontario: 349– 354.
- SAVAGE, S. B. & HUTTER, K. (1989) - *The motion of a finite mass of granular material down a rough incline.* J. Fluid Mech., **199**: 177– 215.
- SAVAGE, S. B. & HUTTER, K. (1991) - *The dynamics of avalanches of granular materials from initiation to runout, part I. Analysis,* Acta Mech., **86**: 201– 223.
- SAVAGE, S. B. & LUN, C. K. K. (1988) - *Particle size segregation in inclined chute flow of dry cohesionless granular solids,* J. Fluid Mech. **189**: 311-335.
- SILBERT, L., ERTAS, D., GREST, G., HALSEY, T., LEVINE, D. & PLIMPTON, S. J. (2001) - *Granular flow down an inclined plane: Bagnold scaling and rheology.* Phys. Rev. E, **64**: 051302.
- STOCK, J. D. & DIETRICH, W. E. (2006) - *Erosion of steepland valleys by debris flows,* Geol. Soc. Am. Bull., **118**(9/10): 1125–1148.
- TANAKA, H., MOMUZU, M., OIDA, A. & YAMAZAKI, M. (2001) - *Simulation of Soil Deformation and Resistance at the Bar Penetration by the Distinct Element Method.* J. Terramechanics, **37**: 41-56.
- TARUMI, Y. & HAKUNO, M. (1988) - *A granular assembly simulation for the dynamic liquefaction of sand.* Natural Disaster Science, **10**(1): 45-59.
- THOMAS, P. A. & BRAY, J. D. (1999) - *Capturing nonspherical shape of granular media with disk clusters.* J. Geotech. and Geoenv. Eng., **125**(3): 169-178.
- TING, J. M., MEACHUM, L. & ROWELL, J. D. (1995) - *Effect of Particle Shape on the Strength and Deformation of Mechanism of Ellipse-Shaped Granular Assemblages.* Eng. Comp., **12**: 99-108.
- TSUJI, Y., TANKA, T. & ISHIDA, T. (1992) - *Lagrangian Numerical Simulation of Plug Flow of Cohesionless Particles in a Horizontal Pipe.* Powder Tech., **71**: 239-250.
- ULLIDTZ, P. (2001) - *Distinct Element Method for study of failure in cohesive particulate media.* Transportation Research Record: Journal of Transportation Research Board, No 1757, Transportation Research Board of the National Academies, Washington, D.C., 127-133.
- WANG, G. & SASSA, K. (2003) - *Pore-pressure generation and movement of rainfall-induced landslides: effects of grain size and fine-particle content.* Eng. Geol., **69**:109-125.
- YOHANNES, B. (2008) - MS Thesis, University of Minnesota, Minneapolis, MN.
- YOHANNES, B. & HILL, K. M. (2010) – *Rheology of dense granular mixtures: particle-size distributions, boundary conditions, and collisional time scales.* Phys. Rev. E **82**(6):060012 (in production).
- ZEGHAL, M. (2001) - *Effect of Particle Shapes on the Resilient Behavior of Aggregate Materials.* Canadian Society of Civil Engineering Annual Conference. Victoria: 1-5.